

CrystEngComm

Accepted Manuscript



This is an *Accepted Manuscript*, which has been through the Royal Society of Chemistry peer review process and has been accepted for publication.

Accepted Manuscripts are published online shortly after acceptance, before technical editing, formatting and proof reading. Using this free service, authors can make their results available to the community, in citable form, before we publish the edited article. We will replace this *Accepted Manuscript* with the edited and formatted *Advance Article* as soon as it is available.

You can find more information about *Accepted Manuscripts* in the [Information for Authors](#).

Please note that technical editing may introduce minor changes to the text and/or graphics, which may alter content. The journal's standard [Terms & Conditions](#) and the [Ethical guidelines](#) still apply. In no event shall the Royal Society of Chemistry be held responsible for any errors or omissions in this *Accepted Manuscript* or any consequences arising from the use of any information it contains.

Solvent mediated phase transformation between two tegafur polymorphs in several solvents.Raitis Bobrovs^{1,2*}, Linda Seton² and Andris Actiņš¹¹ Faculty of Chemistry, University of Latvia, Kr. Valdemara iela 48, Riga, LV-1013, Latvia² Formulation and Drug Delivery Research Group, School of Pharmacy and Biomolecular Sciences, Liverpool John Moores University, Liverpool, L3 3AF, UK

E-mail: raitis.bobrovs@lu.lv

Phone: +371 67372576

Abstract

This paper describes a study of the solvent mediated polymorphic transformation (SMPT) of the metastable α tegafur to the thermodynamically stable β tegafur in several solvents. Phase transformation in acetone, ethanol, *i*-propanol, toluene, and water at 22 °C were described with the solid state kinetic model P2, and rate constants for this process were in the range from 0.028 min⁻¹ to 0.0056 min⁻¹. In all the employed solvents an induction time was observed. Kinetic, solubility and scanning electron microscopy data indicated that nucleation kinetics corresponded to second-order power function and, according to the kinetic model, nuclei growth rate was constant in the examined SMPT. Surface nucleation was observed, and possible nucleation mechanism was given. The phase transition rate depended linearly on the difference between the equilibrium solubilities of α and β tegafur in the respective solvent, i.e. supersaturation.

Introduction

Different crystalline forms of the same molecular entity are known as polymorphs. Polymorphism is a very common phenomenon in chemical manufacturing, for example, in pigment, food and, most of all, in the pharmaceutical industry¹, where at least two thirds of active pharmaceutical compounds have more than one solid form²⁻⁵. One of the tasks for the pharmaceutical industry is to find and select the solid forms with the optimal characteristics for the intended use, because the solubility, dissolution rate, and bioavailability of drug substances are influenced by polymorphism. Therefore it is a common requirement in the pharmaceutical industry that a manufactured compound must be in one, strictly defined crystalline phase^{3,5}. To ensure product stability, the thermodynamically stable polymorph in ambient conditions is normally chosen for manufacturing. However, due to enhanced dissolution or bioavailability profiles, a metastable form might be chosen for manufacturing. To ensure that polymorphs do not

transform over time, the polymorphic stability must be evaluated with respect to ambient, storage, and packaging conditions. The stability of polymorphs under certain temperature and pressure conditions is defined by their free energy, with the most stable polymorph having the lowest free energy in the given conditions³⁻⁵.

Crystallization is the most common method of chemical compound isolation from solution on a manufacturing scale, and it is governed by a combination of thermodynamic and kinetic factors³⁻⁶. Crystallization of polymorphs often follows Ostwald's rule of stages⁷, which postulates that crystallization in a polymorphic system progresses from supersaturated state to equilibrium state in stages. Thus, according to Ostwald's rule of stages, the metastable form should crystallize first and then the system should move through each possible polymorphic structure before the thermodynamically stable polymorph crystallizes. In the majority of cases the thermodynamically stable polymorph in given conditions is isolated, however, the solvent used for crystallization can affect the crystallization outcome and it might promote the crystallization of a specific metastable polymorph. The metastable polymorph will attempt to transform to the stable form if possible, and therefore it is important to study polymorphic transformation 'reactions' to determine the factors influencing the outcome of a polymorphic crystallization. One type of polymorphic transformation 'reaction' drawing attention is solvent mediated polymorphic transformation (SMPT)^{4,8-10}. This is a process, where the metastable polymorph interacts with a bulk solvent phase, and gradually transforms to the more stable polymorph by a process of dissolution and crystallization. SMPT is interpreted as a three-step process – dissolution of the metastable phase, nucleation of the stable phase, and growth of the stable phase^{11,12}. The driving force in this process is the difference between the solubilities and dissolution rates of both polymorphs, which consequently determines the supersaturation level during the crystallization of the thermodynamically stable form. SMPTs have been extensively studied over the years^{8,9,13-30}, however, there are no comprehensive studies on the choice of solvent on the SMPTs. Such studies might be useful for pharmaceutical industry in order to use SMPTs in pharmaceutically active compound manufacturing. SMPTs can be used to produce the thermodynamically stable polymorph if crystallization from a solvent gives a metastable polymorph. On the other hand, if a metastable polymorph is desired, knowledge of possible SMPTs of the respective system is important, because there might be situations when metastable polymorph crystallizes, and through unwanted SMPT subsequently transforms to the thermodynamically stable polymorph.

Here we study SMPT of the metastable α tegafur to the thermodynamically stable β tegafur in several popular solvents from different solvent classes: aprotic polar, aliphatic aprotic apolar,

hydrogen bond donor and aromatic apolar. Both polymorphs of tegafur are produced commercially; therefore knowledge of this polymorphic system SMPTs might be relevant for pharmaceutical industry. The pharmaceutically active compound used in this research, tegafur (5-fluoro-1-(tetrahydrofuran-2-yl)pyrimidine-2,4(1*H*,3*H*)-dione) (Figure 1), is an antitumor agent, widely used in the treatment of various malignancies, particularly gastrointestinal and breast cancers³¹. Over many years the α , β , δ , γ and ε forms of tegafur have been reported in the pharmaceutical literature³¹⁻³³, but only the α and β modifications are used for therapeutic purposes.

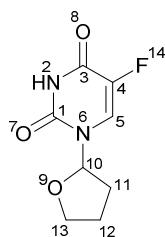


Figure 1. Molecular structure of tegafur (5-fluoro-1-(tetrahydrofuran-2-yl)pyrimidine-2,4(1*H*,3*H*)-dione).

1. Materials and methods

1.1. Materials

Commercial samples of the α and β tegafur were supplied by JSC Grindeks (Latvia). Acetone, cyclohexane, ethanol, *i*-propanol, and toluene of analytical grade were purchased from commercial sources, and deionized water (electrical conductivity $<0.1\mu\text{S}$) was prepared by Adrona, Crystal 5 (Latvia). Solvents were used without further purification. All of the reagents used were certified $>99\%$ pure.

1.2. Methods

1.2.1. Solvent mediated polymorphic transformations

The SMPT was investigated in acetone, cyclohexane, ethanol, *i*-propanol, toluene, and water. Slurrying was performed in Erlenmeyer flasks, where 0.5 g of α and β tegafur mixture at the weight ratio of 1:1 was added to 5 mL of solvent, and suspended for 5 min, 30 min, 3 h, and 72 h at room temperature ($22\pm 1^\circ\text{C}$). The mixture of α and β tegafur was weighed on an analytical balance (BOECO, Germany, $d = \pm 0.0001\text{ g}$), and homogenized by shaking for 5 min in a Retsch

MM 300 shaker (Retsch GmbH, Germany) with the shaking frequency of 10 Hz. Slurrying was performed using an orbital shaker, Biosan OS-10 (Latvia) at a stirring rate of 200 rpm.

The transformation of α tegafur to the stable β tegafur was monitored and quantified via *ex-situ* powder X-ray diffraction (PXRD) analysis. Quantification of the polymorphic composition for the dry residue was carried out as described in Section 1.2.3.

In order to assess the impact of sample suspension and sample drying on the phase transition, comparison experiments were performed, where α and β tegafur mixtures were placed in glass PXRD sample holders (~ 0.2 g) and moistened with the appropriate solvents (100 μ L) using a micropipette (± 0.3 μ L). Sample compositions were quantified using PXRD.

Analogous experiments were performed with pure metastable α tegafur to ensure that such treatment does not promote phase transition even for samples without β tegafur impurities.

1.2.2. *The kinetics of solvent mediated polymorphic transformations*

Acetone, ethanol, *i*-propanol, toluene, and water solutions (~ 100 mL) saturated with respect to α tegafur were prepared by stirring excess α tegafur for ~ 3 h at 22 ± 1 °C. The excess tegafur was filtered off and the clear solution was used for SMPT. In order to ensure that the solution was saturated with respect to α tegafur, PXRD patterns of filtrates were recorded. Solution concentration was determined as described in Section 1.2.5.

SMPT kinetics experiments were performed at 22 °C in a thermostated (Grant TC120, an accuracy ± 0.1 °C; England) glass flow-through cell (250 mL) with a magnetic stirrer. 1.0 g of α tegafur (used as received) was added to the saturated solution and the solid phase was monitored every 10 min for a period of 2 h throughout the transformation. The stirring of the slurry was stopped for 20 seconds to allow the suspended solid particles to settle. Solid phase samples (~ 10 mg) for polymorphic composition determination were collected with a metal spoon from the suspension. The collected solid phase was quickly filtered through a 2-3 μ m filter paper using a glass filter funnel with Buchner flask under reduced pressure. The quantity of α tegafur in the sample was monitored and quantified via *ex-situ* powder X-ray diffraction (PXRD) analysis. The PXRD patterns for dry samples were recorded and analyzed as described in Section 1.2.3.

The tegafur concentration in solution was measured every 20 to 40 min throughout SMPT. Samples for solution concentration measurements were gathered at the same time as solid phase samples for polymorphic composition determination were collected. Approximately 2 mL of saturated solution was filtered through a 0.20 μ m syringe filter and then 1.00 mL of clear solution

was transferred to a preweighed vial with micropipette ($\pm 10 \mu\text{L}$). The solution was left to evaporate at room temperature, weighed and the tegafur solubility was calculated. Two parallel experiments were performed.

1.2.3. The PXRD analysis

The samples were analyzed with a Bruker D8 Advance and Bruker D8 Discover powder X-ray diffractometers (Bruker AXS, Karlsruhe, Germany), equipped with a PSD *LYNXEYE* detectors. The measurements were performed with $\text{Cu K}\alpha$ radiation (1.54180 \AA) at room temperature. The following conditions were used: step-scan mode with a step size of 0.02° ; scan speed: $0.2^\circ/\text{min}$; 2θ range: $8.0^\circ - 20.0^\circ$; voltage: 40 kV; current: 40 mA; divergence slit: 0.6 mm; anti-scattering slit: 8 mm.

PXRD calibration was performed using mixtures of 5.0 %; 10.0 %; 20.0 %; 50.0 %; 80.0 %; 90.0 % and 95.0 % β tegafur in α tegafur ($\sim 0.3 \text{ g}$ total sample weight). The mixtures were weighed using an analytical balance and samples were homogenized by shaking for 5 min in a Retsch MM 300 shaker with the shaking frequency of 10 Hz. The powder samples were packed into glass holders and pressed by a glass slide to ensure coplanarity of the powder surface with the surface of the holder.

The quantitative phase analyses were performed using fundamental parameter based Rietveld software BGMN³⁴. Structure data necessary for quantitative analysis were acquired from the Cambridge Structural Database (CSD) structures with the reference codes BIPDEJ for α tegafur and BIPDEJ02 for β tegafur.

PXRD patterns for calibration samples, and samples collected from experiments were recorded and analyzed identically.

1.2.4. Scanning electron microscopy (SEM)

SEM imaging was performed using Quanta 200 SEM (FEI, Holland) system. Samples were initially gold coated using a K550X sputter coater (EMITECH, UK) and subsequently scanned using an acceleration voltage of 5.0 kV at a working distance of approximately 10 mm. SEM analyses were performed for the same samples that were used for PXRD analysis.

1.2.5. Tegafur solubility measurements

An excess amount of the thermodynamically stable β tegafur was added to 15 mL of acetone, cyclohexane, ethanol, i-propanol, toluene, and water, and was left to stir overnight at 22 ± 1 °C. The saturated solution was filtered through a 0.20 μm syringe filter and then 10.0 mL of clear solution was transferred to a preweighed vial. Solution was left to evaporate at room temperature, weighed and tegafur solubility was calculated. Solubility of the metastable α tegafur was determined identically, except solutions were stirred for ~ 3 h at 22 ± 1 °C, in order to prevent phase transformation to the thermodynamically stable β tegafur. PXRD patterns of filtrate were recorded to ensure that the solubility of the desired polymorph was determined. Two parallel experiments were performed.

1.2.6. Crystallographic face indexing

Crystallographic face indexing was undertaken using single crystal X-ray diffractometer Nonius Kappa CCD diffractometer (Bruker AXS, Karlsruhe, Germany) with Mo K_{α} radiation (0.71073 Å) at 60 kV and 30 mA. Data were collected at room temperature. Face indexing was performed using *Collect* software³⁵.

2. Results and discussion

2.1. The characterization of starting materials

The α and β forms of tegafur were analyzed using PXRD and were confirmed to have equivalent peak positions to those simulated from crystal structure data (CSD, reference codes BIPDEJ and BIPDEJ02) (Figure 2). No impurities of other polymorphs or any contamination were detected in the starting materials. A preferred crystal orientation was observed for α tegafur, because of its needle-like crystal morphology. Typical crystal shapes of both polymorphs are given in Figure 3.

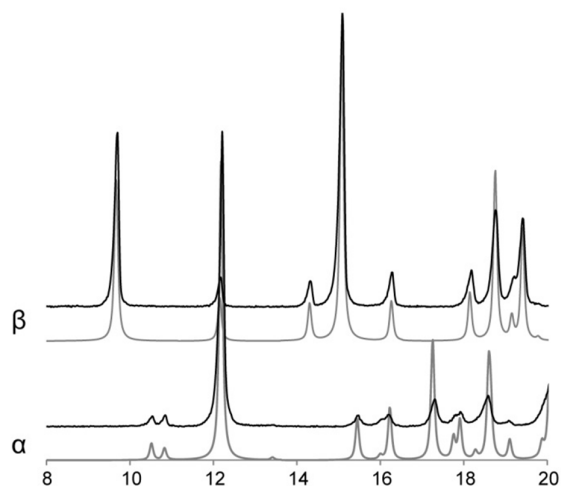


Figure 2. The experimentally measured (black line) and calculated (grey line) PXRD patterns of α and β tegafur.

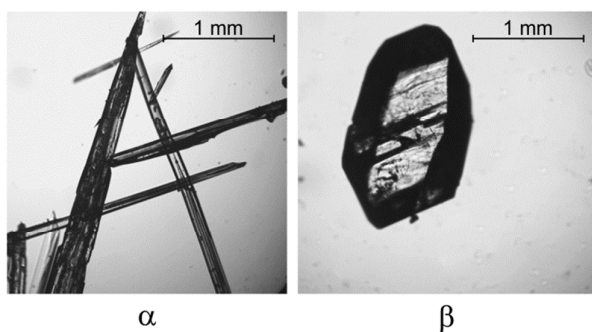


Figure 3. Photomicrographs of α and β tegafur crystals.

Table 1. Crystallographic information of α and β tegafur³⁶.

	α tegafur	β tegafur
System	triclinic	monoclinic
Space group	P -1	P 2 ₁ /n
a, Å	8.994(8)	11.891(5)
b, Å	16.612(9)	14.556(2)
c, Å	5.981(5)	5.062(1)
α , °	86.40(6)	90
β , °	94.06(15)	99.05(2)
γ , °	80.29(8)	90
Z	4	4

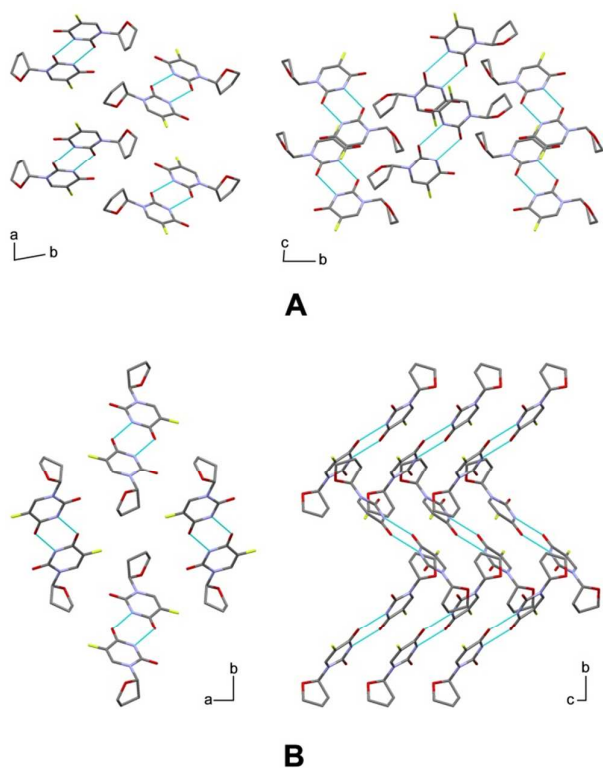


Figure 4. Crystal packing of (A) α tegafur and (B) β tegafur. Hydrogen atoms are omitted for clarity.

Crystallographic information of α and β tegafur is given in Table 1. The base motif of α and β tegafur crystal structures is a tegafur molecule dimer with a $R_2^2(8)$ motif where tegafur molecules are connected via two N2-H \cdots O7 hydrogen bonds (Figure 4). The dimers are not identical in both polymorphs, because the crystal structure of α tegafur consists of two conformationally different molecules (A and B), whereas β tegafur has one molecule in its asymmetric unit and conformation of this molecule matches the conformation of molecule B in α tegafur³⁷. Dimers in α tegafur are formed between conformationally identical molecules, that is, one α tegafur dimer is formed by two A molecules, and the second by two B molecules. Tegafur dimers in the α polymorph are cross-linked by weak C5-H \cdots O9 and C11-H \cdots O8 hydrogen bonds, whereas in β tegafur dimers are stabilized by weak C5-H \cdots O7 and C12-H \cdots F14 hydrogen bonds. It is worth noting that tegafur dimers in α form forms between the same enantiomers (there are two enantiomerically and conformationally different dimers), whereas in β tegafur dimers forms between two enantiomerically different molecules³⁷. Crystallographic face indexing of α tegafur crystals (see Section 2.4) indicated that crystal growth along the a axis is promoted. This is because of

relatively easy tegafur dimer access to the growing surface and the possibility to form multiple weak hydrogen bonds between F14, O8, O9 and C5-H, C11-H. Hydrogen bonds in β tegafur are distributed more evenly and they are stronger than in α tegafur. The same groups are involved in hydrogen bonding for β tegafur, with the difference that instead of C11-H hydrogen, C12-H forms hydrogen bond with fluorine atom. Hydrogen bonding in β tegafur enables cross-linked *zigzag chains* in the *b* direction, however no preferred crystal growth orientation is observed for β tegafur.

2.2. Quantitative phase analysis

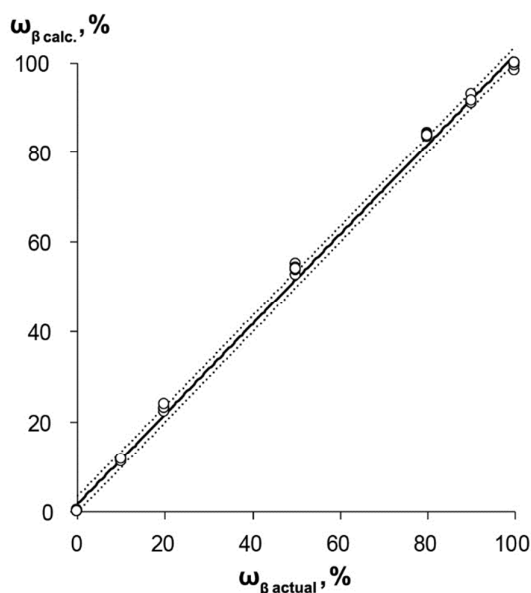


Figure 5. The dependence of calculated β tegafur weight fraction ($\omega_{\beta \text{ calc.}}$) upon the actual β tegafur content in the sample ($\omega_{\beta \text{ actual}}$). Statistical probability $p < 0.05$.

The calibration curve of α and β tegafur mixture is given in Figure 5. The homogenous composition of the analysed mixtures and equivalent extinction effects for both polymorphs should ensure that the diffraction peak intensity of each phase depends linearly on the phase weight fractions in the sample³⁸. It is evident that the correlation was not completely linear and the calculated content of β tegafur in the samples was up to 2 % higher than was actually weighed. We believe that this was because of the preferred orientation of α tegafur, different degree of crystallinity for both polymorphs and possible microabsorption. Nevertheless, experimental data can be described with linear equation $y = (1.02 \pm 0.01) x$, with R^2 value of 0.9990. The method used was found to be linear in the range 0 – 100 % with limit of detection (LOD) and limit of

quantification (LOQ) calculated³⁹ to be 3.0 and 9.2 %, respectively. The method was found to be precise with relative standard deviation (RSD) of 2.0 %. Statistical probability (p) used was $p < 0.05$. Relatively high LOD, LOQ and RSD values are because of the fast scan speed (0.2 °/min) used in the experiments. In order to maintain consistency, scan speed used for calibration was the same as further used in SMPT quantitative analysis. Scan speed of 0.2 °/min was chosen because of the ability to provide fast PXRD measurements necessary for kinetic SMPT studies.

2.3. Solvent mediated polymorphic transformations

Initially SMPT experiments for α and β tegafur mixture with the weight ratio of 1:1 were performed to estimate the approximate phase transition rate. The results of the slurry bridging experiments showed that in all the employed solvents the metastable form converted into the thermodynamically stable form. The weight fraction of β tegafur in the starting material was 50 ± 2 %. The weight fractions of β tegafur in the samples after slurry bridging experiments with various solvents are given in Figure 6.

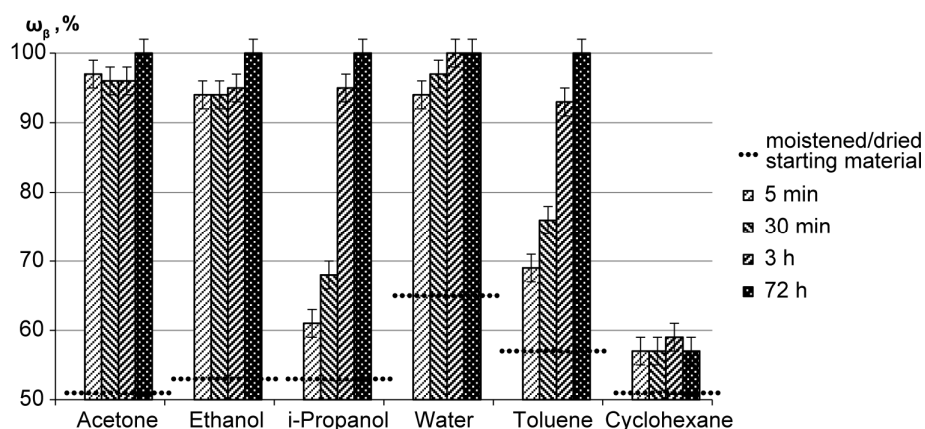


Figure 6. The weight fraction of β tegafur in the samples after slurring a 1:1 mixture of α and β tegafur for 5 min, 30 min, 3 h and 72 h in acetone, ethanol, *i*-propanol, water, toluene, and cyclohexane. Dashed line (---) represents the weight fraction of β tegafur in the sample after the experiment, where no slurring was performed and the sample was only moistened and dried in ambient temperature (indicated as “moistened/dried starting material”).

It is known^{3,5,40–42} that substantial phase transition from one phase to another in a polymorph mixture can be promoted even by a solvent addition (without any external influence). This is because both polymorphs of the substance dissolve in the solvent added and then the stable polymorph in the given conditions will crystallize. In order to evaluate the impact of residual

solvent on SMPT during the drying, experiments where samples were only moistened and dried were performed. The weight fractions of β tegafur after these experiments are given in Figure 6 and are indicated as “moistened/dried starting material”.

Experiments showed that phase transformation took place over a period of time which varied across the solvents studied. Almost complete phase transition to the thermodynamically stable β polymorph was observed in acetone, ethanol, and water after only 5 min of slurring. The phase transition was slower in *i*-propanol and toluene, and complete phase transition to the β polymorph was observed only after more than 3 h of slurring. Minor changes (<10%) in the weight fraction of β tegafur were observed for samples slurried in cyclohexane for 3 days. We believe that no or only minor phase transition occurred in cyclohexane because of its aprotic apolar nature and the negligible solubility of tegafur in this solvent. It is also possible that the observed negligible weight fraction changes in cyclohexane could be related to sample homogeneity and accuracy of PXRD method (RSD = 2.0 %).

As previously mentioned, the experiments where no slurring was performed, but sample was only moistened and dried, were carried out for comparison purposes. This procedure gave a major increase in the weight fraction of β tegafur for samples that were moistened with water and toluene, but for samples that were moistened with acetone, cyclohexane, ethanol, and *i*-propanol increase in the weight fraction of β tegafur were minor. One of the explanations for such results could be as follows. As previously mentioned, SMPTs are considered as three-step processes consisting of the dissolution of the metastable phase, nucleation of the stable phase, and growth of the stable phase. All these stages and, hence, the phase transition extent are affected by the solvent and solid phase interaction time; therefore it is possible that phase transition extent was affected by the solvent evaporation time. Acetone, ethanol, and *i*-propanol are relatively volatile compared to water and toluene, and accordingly, the phase transitions in acetone, ethanol, and *i*-propanol had less time to occur. In order to understand solvent effect on studied SMPT, and to find out factors affecting this phase transformation, more detailed phase transformation kinetics experiments were performed.

2.4. The kinetics of solvent mediated polymorphic transformations

During our first SMPT kinetics experiments we noticed that the sample drying time had an impact on the extent of phase transition – samples, dried at ambient temperature, had increased β tegafur content. This was because the thermodynamically stable β tegafur crystallized from the

saturated tegafur solution that was sampled together with the solid phase, i.e., phase transition to β tegafur partially occurred during sample drying, not only during the slurring. In order to avoid this effect, samples for SMPT kinetic experiments were quickly filtered using a glass filter funnel with Bunsen flask under reduced pressure.

Kinetics experiments with cyclohexane were not performed, since only negligible changes in the β tegafur weight fraction during slurring in cyclohexane were observed in the previous experiments.

For a further data analysis it is worth mentioning that in the previously discussed experiments samples were treated with pure solvents, but in kinetics experiments tegafur-saturated solvents were used to separate tegafur dissolution effects.

The results of the kinetics experiments performed at room temperature (22 ± 1 °C) represent a series of plots documenting the composition of the solid phase during the SMPT, as detected with the PXRD method. Figure 7 shows the composition of the solid phase during the SMPT in acetone, ethanol, *i*-propanol, toluene, and water. These data were used to generate an additional data plot where phase transition kinetics curves were normalized to the state where a complete transition to β tegafur was observed (Figure 8). This means that the time when a complete phase transition was observed was considered as 100%. Using this approach we could compare the reaction rate and reaction path in all the solvents used. This figure clearly demonstrates that the phase transition models were the same in all the solvents, and the only factor that changed was the phase transition rate. An induction time was observed at the beginning of phase transitions in all solvents. We cannot clearly assure whether the observed delay of the phase transition is an induction time or the time that is necessary for β tegafur crystals to grow; however, we believe that this was the limiting step in investigated SMPTs. We see that the induction times in all the solvents were proportionally the same – about 10% of the phase transition time. It is worth noting that the LOD of our quantitative analysis method was 3.0 %, therefore the observed induction time might be the time that was necessary to overcome this 3.0 % range.

Solution concentration throughout SPMT stayed at the level of α tegafur solubility, and started to decay only when all α tegafur transformed to the stable β tegafur (Figure 9). This means, that the overall rate of consumption of supersaturation by β tegafur crystal growth was lower than the overall rate of α tegafur dissolution. This case is denoted as “nucleation-growth controlled polymorphic transformation”¹⁶.

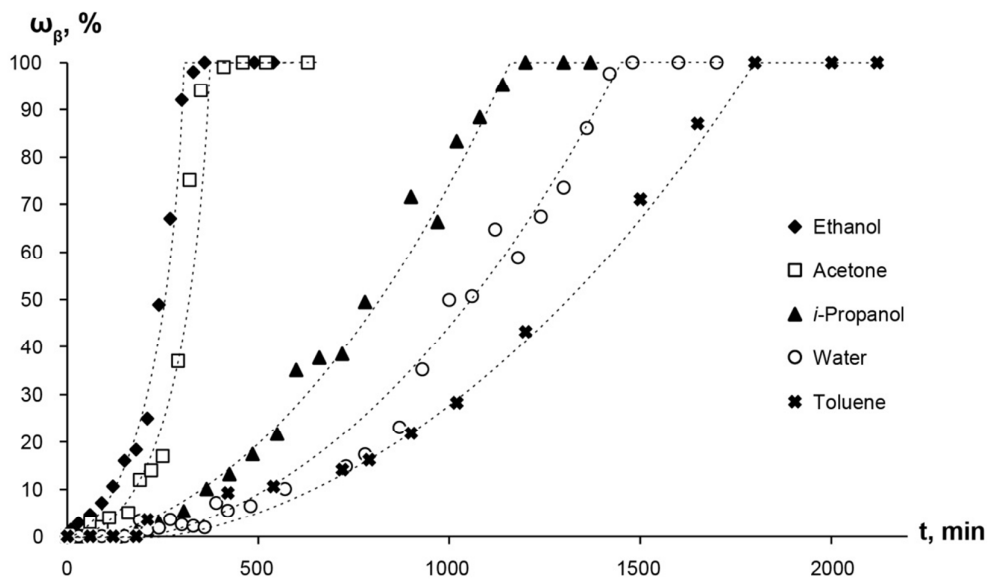


Figure 7. The weight fraction of β tegafur during the SMPT from α tegafur to β tegafur in acetone, ethanol, *i*-propanol, toluene, and water at 22 °C. Line added as a guide.

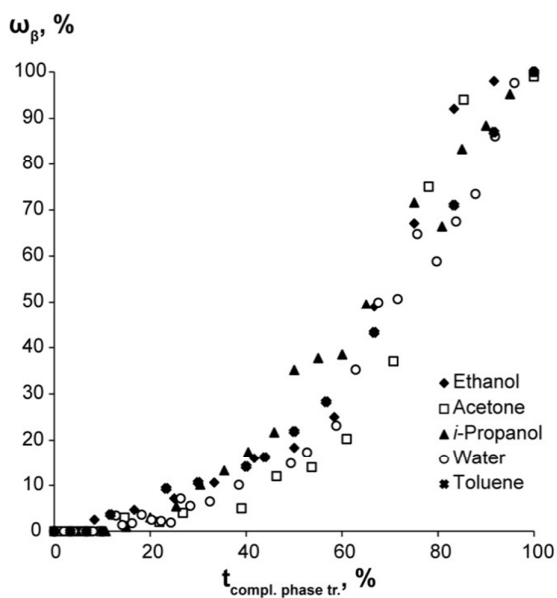


Figure 8. The weight fraction of β tegafur during the SMPT in acetone, ethanol, *i*-propanol, toluene, and water at 22°C, normalized to the state where the transition to β tegafur is complete.

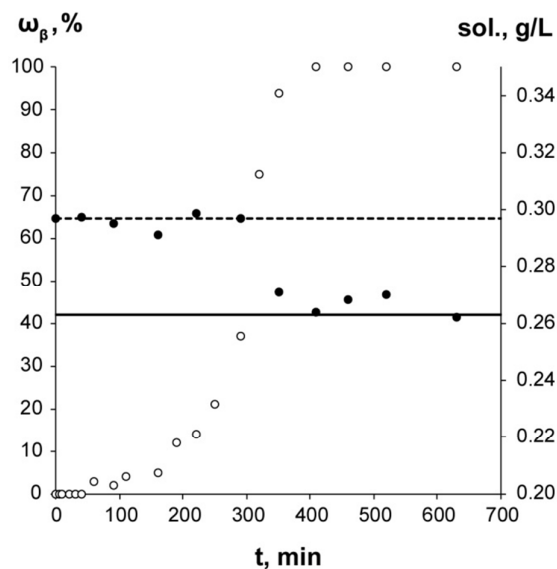


Figure 9. Solution concentration (●), and weight fraction of β tegafur in the solid phase (○) during the SMPT from α tegafur to β tegafur in acetone at 22 °C. The dashed line (---) represents the solubility of α tegafur, continuous line (—) represents the solubility of β tegafur.

The induction time was followed by a gradual increase of the thermodynamically stable β tegafur fraction. SEM analysis of the sample, where β tegafur was first detected using PXRD method, revealed that the blocky β tegafur crystal were in contact with the surface of α tegafur needle-like crystal side faces (Figure 10). Although it is possible that α and β tegafur crystals simply agglomerated together during the sample filtration and drying, the fact that it was not possible to separate these crystals without damaging them, indicated that β tegafur, most likely, nucleated epitaxially on the surface of α tegafur. Observed epitaxially driven polymorphic transformations are common in SMPTs^{8,9,14,21,23,25,43}. The surface of the α tegafur here acted as a nucleation substrate for the β tegafur by either decreasing the solution-nucleus interfacial energy, by topographical contribution or by a crystal lattice match⁹. The surface nucleation might have also been a consequence of a local lattice disorder or amorphous region that had similarity to crystallizing β tegafur⁸.

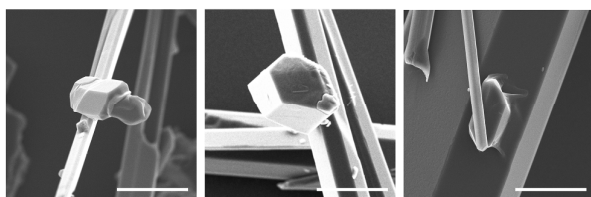


Figure 10. SEM images of the solid phase of SMPT in acetone taken at 60 min. Scale bar 40 μm .

In order to estimate the nucleation mechanism and understand which α and β tegafur crystal faces were in contact, crystal face indexing was performed for both polymorphs. Crystals, where β tegafur was in contact with α tegafur (like those in Figure 10), were not suitable for β tegafur crystal face indexing, therefore individual β tegafur crystals were indexed. Crystals for β tegafur face indexing were collected at 300 min, when individual β tegafur crystals suitable for crystal face indexing were in the sample. Appropriate β tegafur crystals were picked out from the phase mixture. Face indexing of α tegafur crystals were performed for sample collected at 60 min.

SEM images showed that β tegafur nucleated on one of the needle-like crystal side faces, while crystallographic face indexing of α tegafur crystal (Figure 11.A) indicated that these faces were $\{001\}$, $\{011\}$ and $\{010\}$. A visual comparison of epitaxially nucleated β tegafur crystal morphology and indexed crystal morphology (Figure 11.B) indicated that crystal face family $\{100\}$, $\{110\}$ or $\{010\}$ must be in contact with α tegafur surface. Intermolecular distance and molecule alignment analysis along these faces revealed that there was a good agreement at a molecular level between the $\{110\}$ face of β tegafur and $\{010\}$ face of α tegafur crystal (Figure 12), while no match was observed along other crystal faces. Possible lattice match between $\{100\}$, $\{110\}$ and $\{010\}$ face of β tegafur and $\{001\}$, $\{011\}$ and $\{010\}$ face of α tegafur was examined using EpiCalc 5.0 software⁴⁴. The lattice matching calculations indicated that there was no lattice matching between any of the studied faces (EpiCalc data can be found in the Supporting Information).

However, it should be taken into account that crystal surface molecules are not static – they change their position, arrangement and conformation^{45,46}, and therefore they could arrange into the state, which promoted the growth of β tegafur. This means that the nucleation of the β tegafur might be favoured by the surface molecule rearrangement. The $\{110\}$ surface of β tegafur and the $\{010\}$ surface of α tegafur have similar tegafur molecule arrangement at the surface and distances between tegafur dimers are the same for both polymorphs in relevant directions. Because of this, nucleation of β tegafur on $\{010\}$ face of α tegafur might be initiated by minor surface tegafur dimer displacement, conformation change, rotation. The strongest hydrogen bond donor and acceptor groups are involved in dimer formation and interactions between dimers are relatively weak. These weak interactions at the growing surface are less efficient at directing the orientation on an incoming dimer synthon and therefore tegafur dimers at the surface are relatively mobile. Figure 13 shows, that tegafur dimer arrangement similar to that in β tegafur, could be achieved by

minor α tegafur surface molecule rotation. Such local lattice disorder would spread and eventually thermodynamically stable β tegafur would nucleate and continue to grow.

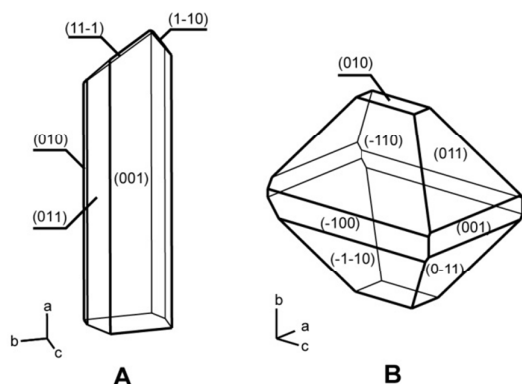


Figure 11. Single crystal face indexing of α and β tegafur.

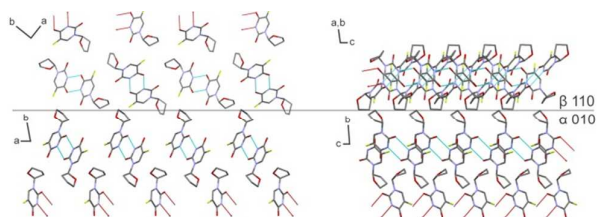


Figure 12. Schematic model of β tegafur growing on the α tegafur surface (010). Hydrogen atoms are omitted for clarity.

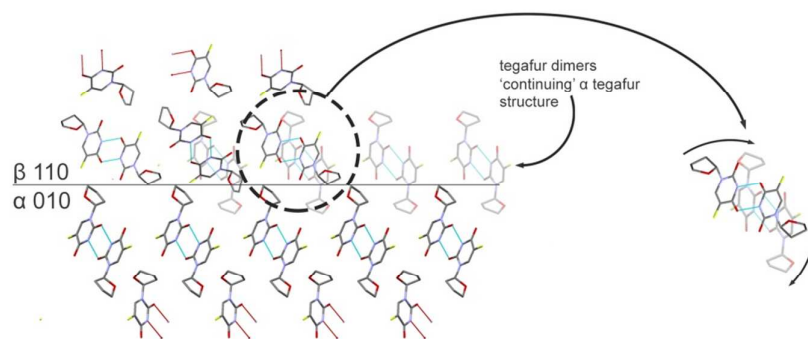


Figure 13. Schematic representation of tegafur dimer rearrangement on the α tegafur surface to initiate the growth of β tegafur. Hydrogen atoms are omitted for clarity.

In order to quantitatively compare SMPT rates in different solvents, experimental data were described with appropriate kinetic model. Solid-state kinetics models are theoretical, mathematical descriptions of experimental data and usually are expressed as rate equations⁴⁷. Many solid-state kinetics models have been developed based on certain mechanistic assumptions, while other models are more empirical and may have little mechanistic meaning. Models currently used in

solid-state kinetic studies are classified according to their mechanistic features, such as nucleation, geometrical contraction, diffusion, and reaction order⁴⁷. SEM imaging of the studied SMPT revealed that the phase transition took place on the solid phase surface (the phase transition was heterogeneous), therefore attempts were made to describe experimental data points with the most common solid-state kinetic models⁴⁷. Evaluation of observed phase transformation nature and crystal growth morphology indicated that experimental data were in agreement with power solid-state kinetics models. The best correlation was observed when the experimental data points were fitted to the power model P2:

$$\alpha = (kt)^2 \quad (1),$$

where k is the phase transition rate constant, α is the weight fraction of β tegafur in sample, and t is time. The correlation of the experimental data with the theoretical model and phase transition rate constants in each solvent are given in Table 2. Rate constants were calculated using MS Excel *Solver* optimization software, based on the least squares method^{48,49}.

Table 2. The P2 model rate constants of SMPT and correlation coefficients, depending on the solvent used; the experiment was performed at 22 °C.

Solvent	Rate constant, min ⁻¹	Correlation with P2 model, R ²
Acetone	0.028	0.92
Ethanol	0.023	0.96
<i>i</i> -Propanol	0.0090	0.92
Water	0.0065	0.98
Toluene	0.0056	0.98

The power law model P2 used here assumes that the nucleation rate follows the power law, while nuclei growth is assumed to be constant^{47,50,51}. Nuclei and crystal growth was constant, because it took place through crystallization from saturated α tegafur solution. The limiting step in nuclei growth was the transport of the tegafur molecule to the crystallization zone. Diffusion of tegafur molecules was expected to occur at a constant rate throughout the phase transition, because the studied phase transition occurred in solution, which was saturated with respect to α tegafur (supersaturation was constant during phase transformation). Taking this into account, nuclei growth rate can be assumed to be constant. This means that the rate-controlling step in the examined SMPT was the nucleation. There are two scenarios for nucleation⁵¹. The first option is a simultaneous formation of all nuclei; the second option is that nucleation occurs stepwise, with

nuclei forming over a period of time. SEM imaging (Figure 10) shows that β tegafur crystals, observed in the sample where β tegafur was first detected, had deviations in the crystal size. This indicates that nucleation in the examined SMPT occurred over a period of time. Besides, it is very unlikely that all the nucleation sites would have approximately the same reaction (phase transition) activation energy minimum, which would be necessary for a simultaneous nucleation. Clearly, nuclei formed first at the nucleation sites with the lowest activation energy, and then nucleation gradually spread to the other nucleation sites in a rising activation energy order. Since nuclei and crystal growth was constant, this nucleation behavior can be described with a second-order power function.

The fact that the best experimental and theoretical data correlation was observed for the 2 dimensional model indicates that the phase transition rate most likely was proportional to the surface area of the β tegafur crystals formed⁵¹. With that said, we can conclude that in the examined SMPT β tegafur crystals nucleation corresponds to a second-order power function, their growth rate was constant, and the phase transition rate was proportional to the β tegafur crystal surface area.

Despite the fact that solubility and phase transformation kinetic data suggested that this phase transformation was limited by nucleation, the correlation between SMPT rate constant and the difference between α and β tegafur solubility in the respective solvent was observed: a faster phase transition was observed for the samples slurried in solvents where the difference in polymorph solubilities was high (Figure 14). This trend in the SMPT from α tegafur to β tegafur was described with equation:

$$k = (0.72 \pm 0.07)\Delta sol. + (0.005 \pm 0.001) \quad (2),$$

where $\Delta sol.$ is difference between α and β tegafur equilibrium solubilities in the respective solvent, and k is the rate constant of the SMPT in the same solvent. The correlation coefficient was $R^2=0.97$. This correlation means that the driving force in the studied SMPT was excess concentration above the equilibrium concentration of β tegafur, i.e. supersaturation with respect to β tegafur. Supersaturation provided the necessary driving force to overcome the energy barrier to promote β tegafur nuclei and crystal growth³. In this case supersaturation coincided with the difference between α and β tegafur equilibrium solubility in the respective solvent, because the solution concentration throughout the phase transformation was fixed at the equilibrium concentration of α tegafur. Such solution concentration profile also means that the driving force was constant throughout the SMPT. Higher tegafur supersaturation in the solution promoted faster

phase transformation to the thermodynamically stable β tegafur, because of the increased degree of local organization in the solution necessary for crystallization⁴⁶, and faster tegafur molecule transfer to the crystallization zone (molecules were relatively close). Absolute tegafur solubility and the difference between polymorph solubilities depends on the chosen solvent, however, the free energy (ΔG) difference between polymorphs does not depend on the solvent²⁸. This means that the overall driving force of phase transformation was not dependent on the chosen solvent, and the SMPT rate depended only on the difference between polymorph solubilities (supersaturation). The only SMPT step that might be affected by solvent choice was β tegafur nucleation^{52–55}. Tegafur molecules were solvated in the solution, similar to the surface of molecular aggregates and crystals. In order to nucleate and continue crystallization, tegafur molecules had to be desolvated, and solvent molecules on the nuclei or crystal surface had to be replaced by incoming tegafur molecules. This process, most likely, was affected by the nature of the solvent and its electron donor/acceptor properties, because strong solute-solvent interaction would inhibit desolvation and therefore nuclei growth, while weak solute-solvent interaction would not have a significant impact on nuclei growth.

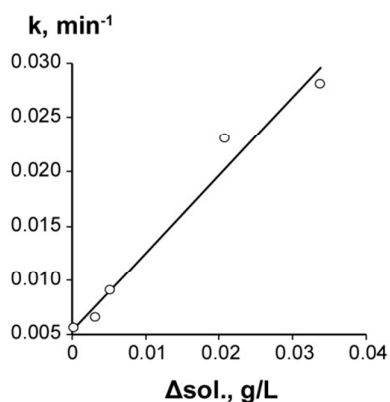


Figure 14. Correlation between SMPT rate constant in acetone, ethanol, *i*-propanol, toluene, and water, and difference between α and β tegafur solubility ($\Delta sol.$) in respective solvent. Correlation equation $y=(0.72\pm 0.07)x+(0.005\pm 0.001)$; $R^2=0.97$.

3. Conclusions

The SMPT from α tegafur to β tegafur in acetone, cyclohexane, ethanol, *i*-propanol, toluene, and water at 22 °C is nucleation-growth controlled and it can be described with the P2 power model. The rate constants for this process were in the range from 0.028 min^{-1} to 0.0056 min^{-1} . In all the employed solvents an induction time (about 10% of the time required for complete phase transition) was observed, indicating that nucleation and/or initial crystal growth was the limiting

factor for SMPTs performed in saturated solutions. In the examined SMPT the nucleation of β tegafur crystals corresponded to second-order power function, nuclei and crystal growth rate was constant, and the phase transition rate was proportional to the β tegafur crystal surface area. Surface nucleation was observed in studied SMPT. Crystal habit investigation indicated that β tegafur nucleated on the $\{010\}$ face of α tegafur, and the $\{110\}$ face of β tegafur was in contact with α tegafur crystal. The SMPT rate depended linearly on the supersaturation level, i.e. difference between α and β tegafur equilibrium solubility in the respective solvent.

4. Acknowledgement

This work has been supported by the European Social Fund within the project “Support for Doctoral Studies at University of Latvia”. Authors acknowledge JSC Grindeks for supplying the α and β polymorphic forms of tegafur. We also acknowledge the Liverpool John Moores University for the possibility to perform SEM imaging and Olga Paškova for carrying out some of the experiments.

5. References

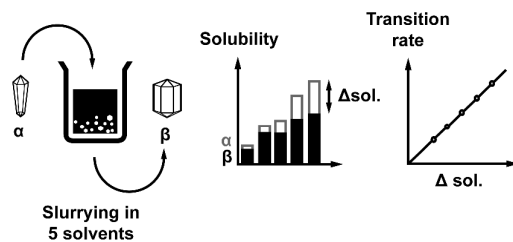
- (1) Bernstein, J. *Polymorphism in Molecular Crystals*; IUCr monographs on crystallography; Oxford University Press, 2007; p. 430.
- (2) Haleblian, J.; McCrone, W. *J. Pharm. Sci.* **1969**, *58*, 911–929.
- (3) Hilfiker, R. *Polymorphism: in the Pharmaceutical Industry*; Hilfiker, R., Ed.; Wiley-VCH: Weinheim, 2006; p. 433.
- (4) Vippagunta, S. R.; Brittain, H. G.; Grant, D. J. W. *Adv. Drug Deliv. Rev.* **2001**, *48*, 3–26.
- (5) Brittain, H. G. *Polymorphism in Pharmaceutical Solids*; Brittain, H. G., Ed.; 2nd ed.; Informa Healthcare USA, Inc.: New York, NY, 2009; Vol. 192, p. 640.
- (6) Caira, M. R. In *Design of Organic Solids*; Weber, E., Ed.; 1998; Vol. 198, pp. 163–208.
- (7) Ostwald, W. *Zeitschrift für Phys. Chemie* **1897**, *22*, 289.
- (8) Murphy, D.; Rodríguez-Cintrón, F.; Langevin, B.; Kelly, R. C.; Rodríguez-Hornedo, N. *Int. J. Pharm.* **2002**, *246*, 121–134.
- (9) Rodríguez-Hornedo, N.; Lechuga-Ballesteros, D. *Int. J. Pharm.* **1992**, *85*, 149–162.
- (10) Rodríguez-Hornedo, N.; Murphy, D. *J. Pharm. Sci.* **1999**, *88*, 651–660.

- (11) Cardew, P. T.; Davey, R. J. *Proc. R. Soc. A Math. Phys. Eng. Sci.* **1985**, *398*, 415–428.
- (12) Davey, R. J.; Cardew, P. T.; McEwan, D.; Sadler, D. E. *J. Cryst. Growth* **1986**, *79*, 648–653.
- (13) Croker, D. M.; Davey, R. J.; Rasmuson, Å. C.; Seaton, C. C. *CrystEngComm* **2013**, *15*, 2044.
- (14) O'Mahony, M. a.; Seaton, C. C.; Croker, D. M.; Veessler, S.; Rasmuson, Å. C.; Hodnett, B. K. *Cryst. Growth Des.* **2013**, *13*, 1861–1871.
- (15) Maher, A.; Croker, D. M.; Rasmuson, Å. C.; Hodnett, B. K.; O'Mahony, M. a. *Cryst. Growth Des.* **2012**, *12*, 1925–1932.
- (16) Maher, A.; Croker, D. M.; Rasmuson, Å. C.; Hodnett, B. K. *Cryst. Growth Des.* **2012**, *12*, 6151–6157.
- (17) Maher, A.; Seaton, C. C.; Hudson, S.; Croker, D. M.; Rasmuson, Å. C.; Hodnett, B. K. *Cryst. Growth Des.* **2012**, *12*, 6223–6233.
- (18) Lehto, P.; Aaltonen, J.; Tenho, M.; Rantanen, J.; Hirvonen, J.; Tanninen, V. P.; Peltonen, L. *J. Pharm. Sci.* **2009**, *98*, 985–996.
- (19) Horst, J. H. Ter; Cains, P. W. *Cryst. Growth Des.* **2008**, *8*, 2537–2542.
- (20) Qu, H.; Louhi-Kultanen, M.; Rantanen, J.; Kallas, J. *Cryst. Growth Des.* **2006**, *6*, 2053–2060.
- (21) Schöll, J.; Bonalumi, D.; Vicum, L.; Mazzotti, M.; Müller, M. *Cryst. Growth Des.* **2006**, *6*, 881–891.
- (22) Aaltonen, J.; Heinänen, P.; Peltonen, L.; Kortejärvi, H.; Tanninen, V. P.; Christiansen, L.; Hirvonen, J.; Yliruusi, J.; Rantanen, J. *J. Pharm. Sci.* **2006**, *95*, 2730–2737.
- (23) Ferrari, E. S.; Davey, R. J. *Cryst. Growth Des.* **2004**, *4*, 1061–1068.
- (24) Maruyama, S.; Ooshima, H. *Chem. Eng. J.* **2001**, *81*, 1–7.
- (25) Cashell, C.; Corcoran, D.; Hodnett, B. K. *Cryst. Growth Des.* **2005**, *5*, 593–597.
- (26) Beckham, G. T.; Peters, B.; Starbuck, C.; Variankaval, N.; Trout, B. L. *J. Am. Chem. Soc.* **2007**, *129*, 4714–4723.
- (27) Ferrari, E. S.; Davey, R. J.; Cross, W. I.; Gillon, A. L.; Towler, C. S. *Cryst. Growth Des.* **2003**, *3*, 53–60.
- (28) Davey, R. J.; Blagden, N.; Righini, S.; Alison, H.; Ferrari, E. S. *J. Phys. Chem. B* **2002**, *106*, 1954–1959.

- (29) Tanoury, G. J.; Hett, R.; Kessler, D. W.; Wald, S. A.; Senanayake, C. H. *Org. Process Res. Dev.* **2002**, *6*, 855–862.
- (30) Saranteas, K.; Bakale, R.; Hong, Y.; Luong, H.; Foroughi, R.; Wald, S. *Org. Process Res. Dev.* **2005**, *9*, 911–922.
- (31) Uchida, T.; Yonemochi, E.; Oguchi, T.; Terada, K.; Yamamoto, K.; Nakai, Y. *Chem. Pharm. Bull.* **1993**, *41*, 1632–1635.
- (32) Actiņš, A.; Beļakovs, S.; Orola, L.; Veidis, M. V. *Latv. J. Chem.* **2006**, *2*, 120–124.
- (33) Needham, F.; Faber, J.; Fawcett, T. G.; Olson, D. H. *Powder Diffraction*. **2006**, *21*, 245–247.
- (34) Bergmann, J.; Friedel, P.; Kleeberg, R. *CPD Newsl.* **1998**, *20*, 5–8.
- (35) Nonius BV; Nonius KappaCCD Collect, 1998.
- (36) Nakai, Y.; Yamamoto, K.; Terada, K.; Uchida, T. In *Proceedings of the 5th symposium on development and evaluation of pharmaceutical preparations*; Naoya, 1983; Vol. 7, p. s–22.
- (37) Nakai, Y.; Yamamoto, K.; Terada, K.; Uchida, T.; Yamaguchi, K.; Shimizu, N. *Chem. Pharm. Bull.* **1986**, *34*, 1242–1248.
- (38) Jenkins, R.; Snyder, R. L. *Introduction to X-ray Powder Diffractometry*; John Wiley & Sons, Inc.: Hoboken, NJ, USA, 1996; p. 432.
- (39) Campbell Roberts, S. N.; Williams, A. C.; Grimsey, I. M.; Booth, S. W. *J. Pharm. Biomed. Anal.* **2002**, *28*, 1149–1159.
- (40) Bobrovs, R.; Petkune, S.; Actiņš, A. *Latv. J. Chem.* **2010**, *1*, 3–16.
- (41) Petkune, S.; Bobrovs, R.; Actiņš, A. *Pharm. Dev. Technol.* **2012**, *17*, 625–631.
- (42) Khoshkhoo, S.; Anwar, J. *J. Phys. D. Appl. Phys.* **1993**, *26*, B90–B93.
- (43) Croker, D.; Hodnett, B. K. *Cryst. Growth Des.* **2010**, *10*, 2806–2816.
- (44) Hillier, A.; Ward, M. *Phys. Rev. B* **1996**, *54*, 14037–14051.
- (45) Tung, H.-H.; Paul, E. L.; Midler, M.; McCauley, J. A. *Crystallization of Organic Compounds: An Industrial Perspective*; John Wiley & Sons, Inc.: Hoboken, NJ, USA, 2009; p. 304.
- (46) Mullin, J. W. *Crystallization*; 4th ed.; Butterworth-Heinemann: Oxford, 2001; p. 600.
- (47) Khawam, A.; Flanagan, D. R. *J. Phys. Chem. B* **2006**, *110*, 17315–17328.
- (48) Bērziņš, A.; Actiņš, A. *J. Pharm. Sci.* **2014**, *103*, 1747–1755.

- (49) Berman, M.; Shahn, E.; Weiss, M. F. *Biophys. J.* **1962**, *2*, 275–287.
- (50) Allnatt, A. R.; Jacobs, P. W. M. *Can. J. Chem.* **1968**, *46*, 111–116.
- (51) Harrison, L. G. In *The Theory of Kinetics*; Compton, R. G.; Bamford, C. H.; Tipper, C. F. H., Eds.; Elsevier Scientific Publishing Company, 1969; Vol. 2, pp. 377–462.
- (52) Musumeci, D.; Hunter, C. a.; McCabe, J. F. *Cryst. Growth Des.* **2010**, *10*, 1661–1664.
- (53) Davey, R. J.; Dent, G.; Mughal, R. K.; Parveen, S. *Cryst. Growth Des.* **2006**, *6*, 1788–1796.
- (54) Kulkarni, S. a; McGarrity, E. S.; Meekes, H.; ter Horst, J. H. *Chem. Commun. (Camb)*. **2012**, *48*, 4983–4985.
- (55) Davey, R.; Garside, J. *From molecules to crystallizers*; Oxford University Press, 2000; p. 96.

A table of contents entry



Here we show that solvent mediated polymorphic transformation rate depends linearly on the difference between equilibrium solubilities of tegafur polymorphs.